ELSEVIER

Journal of Power Sources 64 (1997) 71–80

JOURNAL OF POWER SOURCES

Soaking and formation of tetrabasic lead sulfate

S. Grugeon-Dewaele [a], J.B. Leriche [a], J.M. Tarascon [a], A. Delahaye-Vidal [a,*], L. Torcheux [b], J.P. Vaurijoux [b], F. Henn [b,1], A. De Guibert [b]

[a] *Laboratoire de Réactivité et de Chimie des Solides, URA CNRS 1211, 33 rue Saint Leu, 80 039 Amiens Cedex, France*

[b] *CEAC (Exide Europe), 5–7 allée des Pierres Mayettes, 92 636 Gennevilliers Cedex, France*

Abstract

Soaking and formation (first charge) stages of the Faure process were studied as separate stages from various $4PbO \cdot PbSO_4$ (4BS) precursors (pure tetrabasic lead sulfate or industrial tetrabasic positive active material). The evolution during soaking and formation of the various well-defined 4BS precursors was followed by means of scanning electron microscopy, X-ray diffraction and wet chemical analysis. The following results arise from this approach. The sulfation stage results in the formation of $PbSO_4$ crystals with two completely different morphologies. The first type of $PbSO_4$ crystals nucleate at the 4BS needle surface and this leads rapidly to large polyhedral particles of 2 μm in diameter. The second type of $PbSO_4$ crystals consist of very small interconnected grains (0.2 μm) that result from the slow transformation of the 4BS needle into $PbSO_4$ via a metasomatic process. Since the 2 μm $PbSO_4$ polyhedral particles resulting from the first sulfation process are more difficult to convert into PbO_2, the PbO_2 crystal growth mainly takes place on the second type of $PbSO_4$ small 0.2 μm interconnected crystals. It can be concluded that the 4BS formation route mainly proceeds via the double metasomatic process $4BS \rightarrow PbSO_4 \rightarrow PbO_2$ leading to the textural relationship between PbO_2 and its precursor 4BS. The double metasomatic process gives rise to the same type of macrotexture at 20 and 55 °C with a rigid skeleton and a high porosity. On the other hand, the thickness of the individual PbO_2 grains (i.e. the microtexture) depends on temperature. Very thin interconnected PbO_2 crystals are obtained at 20 °C while thicker grains are observed at 55 °C. These textural observations are confirmed by $C/20$ discharge capacity measurements on tetrabasic-based plates and batteries. The influence of soaking duration is outlined.

Keywords: Basic lead sulfate; Lead/acid batteries; Positive plates

1. Introduction

The processing of the positive plates for lead/acid batteries consists of several steps, each of them involving very complex reaction mechanisms. The first stage consists of the incomplete oxidation of metallic lead into leady oxide (PbO with residual Pb) by the 'Barton pot' or 'mill' processes. A paste is prepared by mixing leady oxide and sulfuric acid, which react to form either tribasic lead sulfate ($3PbO \cdot PbSO_4 \cdot H_2O = 3BS$) or tetrabasic lead sulfate ($4PbO \cdot PbSO_4 = 4BS$) or a mixture of both depending on the experimental conditions (temperature, composition of the mixture). This paste is applied to a lead alloy grid and subjected to curing in a highly humid atmosphere in the 60–80 °C temperature range: during this stage, the remaining metallic lead is oxidized, while the 3BS phase recrystallizes leading to an increase of the 3BS particle size or to the transformation into large elongated prismatic crystals of 4BS. These structural and morphological changes enhance the mechanical strength of the active material and the contact between the mass and the grid. Finally, the first charge, which is denoted formation, takes place. For this stage, two main reactions can be distinguished. First, due to the soaking of the plates in the electrolyte, the basic lead sulfates are partially converted into lead sulfate $PbSO_4$. Simultaneously, the lead or basic lead sulfates (3BS, 4BS, $PbSO_4$) are electrochemically oxidized leading to the charged active material PbO_2.

The structural and textural features of PbO_2 (structural defects, morphology, specific area) which depend on the mechanisms involved during the first charge strongly influence the performance of the batteries. Thus, a better understanding of the cured plate oxidation mechanisms is required in order to optimize the performance of the PbO_2 active material.

Cured plates containing large amounts of 4BS are characterized by good mechanical strength and long cycle life.

* Corresponding author.

[1] Present address: Laboratoire de Physico-Chimie de la Matière Condensée, UMR 5617, Université de Montpellier II, place Eugène Bataillon, 34 095 Montpellier Cedex 5, France.

0378-7753/97/$17.00 © 1997 Elsevier Science S.A. All rights reserved
PII S0378-7753(96)02505-0

These good performances are generally ascribed to the 'metasomatic process' involved during the first charge. According to Burbank [1], during the charge, the large needles of the cured 4BS phase are converted into a large number of fine PbO_2 crystals gathered into agglomerates which retain the initial overall shape of the 4BS crystals. Because of their interlocking structure, this process, referred to as 'metasomatic', allows the porous and rigid character of the plates to be conserved.

Other studies [2–7] confirmed the metasomatic process but all failed to determine, with a great precision, the structural and textural relationships that exist between the initial 4BS, $PbSO_4$ and PbO_2 particles: the soaking and formation stages not being studied separately. Therefore, it was very difficult to evaluate the specific role of the $PbSO_4$ phase (an insulating phase) on the charge performance of the batteries.

More recently, soaking and oxidation mechanisms of cured plates containing 4BS have been separately studied by Lam et al. [8]. They confirmed that during soaking, the large crystals of 4BS are progressively converted into $PbSO_4$ through a metasomatic process. In addition, they proposed mechanisms for 4BS formation reactions, as a function of the soaking time, and they demonstrated that the use of pulsed current conditions improved the efficiency of the formation process. However, the collected data came from industrial plates for which the studies of the active material characterization were difficult, because of the composite nature of the positive electrodes.

In this paper, we compare the behaviour of industrial cured plates containing large amounts of 4BS to own-made plates containing pure 4BS phases of well-defined morphologies during soaking and formation reactions. New textural features which give additional information on the resulting PbO_2 active material are concluded from this comparison.

2. Experimental

2.1. Starting materials

The pure 4BS phases used as starting material were synthesized either by Biagetti's method [2] (sample denoted as $4BS_B$) or by curing of a pure tribasic lead sulfate (sample denoted as $4BS_C$). Biagetti's method consists of mixing lead oxide (PbO) and stoichiometric quantity of a sulfuric acid solution at 80 °C. The resulting powder is then heated to a temperature of 550 °C to increase its purity. This preparation mode leads to large needles of pure $4BS_B$ with length up to 30 μm and a diameter of 3–5 μm, some of them being broken, see Fig. 1(a). Large needles (10 μm × 0.1 mm) are also obtained (Fig. 1(b)) by curing a 3BS sample with PbO (molar ratio 80/20) in water at 100 °C in a polytetrafluoroethylene (PTFE) dish. The starting pure 3BS phase is prepared by the Bode and Voss method according to the detailed procedure given in Ref. [9].

For the industrial active material study, we used automotive positive plates cured at a high temperature. The corresponding positive active material presents large needle-shaped tetrabasic crystals (Fig. 1(c)), length ≈ 100 μm and diameter ≈ 10 μm on ≈ 1.5 mm thick Pb–Sb grids. This material presents between 40 and 50% of residual lead oxide (α-PbO and β-PbO) and around 1% residual of free lead (Pb).

Fig. 1. SEM micrographs of the 4BS starting materials used during the soaking and formation reactions: (a) pure needles prepared according to Biagetti's method ($4BS_B$); (b) 4BS sample prepared by curing of a 3BS precursor ($4BS_C$), and (c) industrial 4BS-type active materials with residual α- and β-PbO and free lead.

2.2. Soaking and formation of pure 4BS phases

For the soaking experiments, the $4BS_C$ and $4BS_B$ powders (300 mg) were dispersed in a large excess (25 cm^3) without agitation in a sulfuric acid solution (sp. gr. 1.23). Samples were removed after various soaking times at room temperature or at 55 °C, rinsed with water and dried under a vacuum pump before X-ray diffraction (XRD) and scanning electron microscopy (SEM) analyses.

For the formation study, the powder (200 mg) was packed with the current collector (diameter: 13 mm) at a pressure of 3 ton cm^{-2}. The current collector consists of a pure-lead pellet previously soaked in a sulfuric acid solution (sp. gr. 1.23) during 24 h. This treatment allowed the pellet to be covered with a film of $PbSO_4$ crystals which were first oxidized in a homogeneous PbO_2 conductive layer during the formation. The positive electrode was then put into a small PTFE cell (swagelock type) with 0.5 ml of sulfuric acid (sp. gr. 1.23), a fibre glass separator and a pure-lead counter electrode (Fig. 2) with an acid/active mass ratio equal to 2.5 $cm^3\ g^{-1}$.

The formation was conducted at room temperature or at 55 °C at a constant current rate ($C/20$) where C represents the theoretical capacity of the 4BS phase, i.e. 224 Ah kg^{-1}. The formed active material was studied by X-ray diffraction

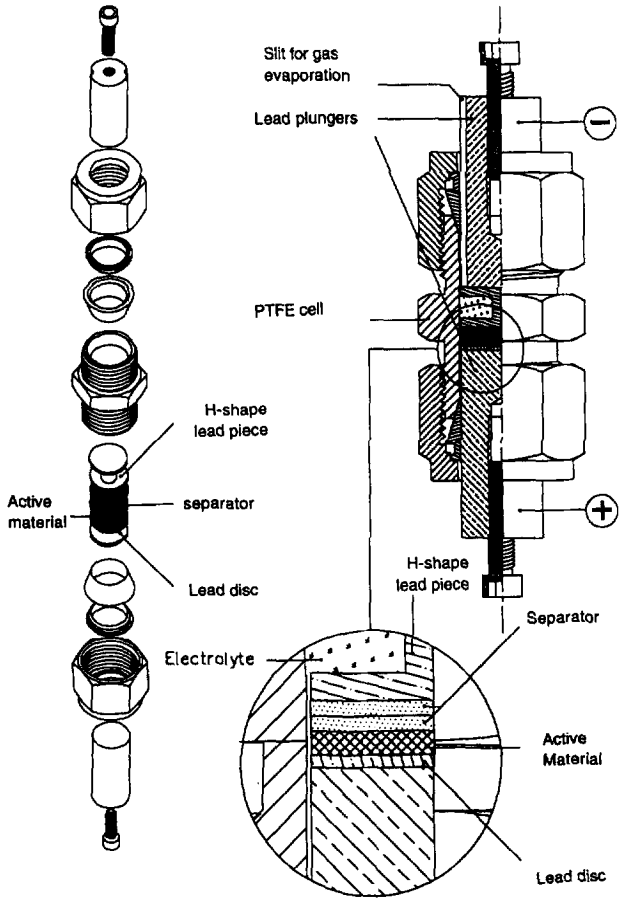

Fig. 2. Swagelok PTFE cell used for the experiment formation of the $4BS_C$ and $4BS_B$ samples.

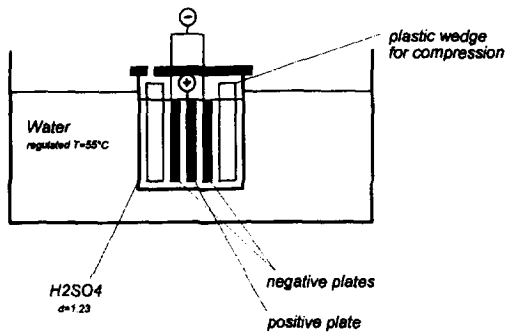

Fig. 3. Experimental set-up for the formation of industrial plates.

at various states-of-charge: 100, 200,300 and 400%. A state-of-charge of 100% at the $C/20$ rate corresponded to a charge of 224 Ah kg^{-1} within 20 h, i.e. 0.56 Ah kg^{-1}.

Depending on the experiments, the formation was performed with a very short soaking treatment (< 1 min) or after 6 h of soaking in a sulfuric acid solution (sp. gr. 1.23).

2.3. Soaking and formation of 4BS industrial plates

Soaking of industrial plates was performed with cured plates in a large excess of sulfuric acid solution (sp. gr. 1.23).

Formation was initiated after the 4BS cured plates being soaked during different times in the following conditions: H_2SO_4 specific gravity = 1.23; acid/material ratio ≈ 3 $cm^3\ g^{-1}$ (large excess of acid). The experimental set-up is given in Fig. 3.

The formation was performed at 320 Ah kg^{-1} during 20 h (143% of the theoritical capacity) with constant current (regime = 0.8 $Ah^{-1}\ kg^{-1}$). The temperature was 55 °C.

2.4. Characterization of soaked and formed active materials

The structural changes of the soaked and formed active material were followed by using the quantitative XRD analysis of the PEAKS program developed by Hill et al. [10]. The XRD patterns were recorded using a Philips diffractometer PW1710 for powder samples and Inel CPS 120 for industrial plates. SEM was performed with a Philips SEM Model 505 (powder samples) or a JEOL-35CF (plates). The plate PbO_2 level was analysed by wet chemical methods. Porosity measurements with a mercury porosimeter were also performed.

3. Results

3.1. Soaking and formation of pure 4BS phases

Soaking of pure 4BS phases was first studied at room temperature and at 55 °C prior to the investigation of the formation reaction.

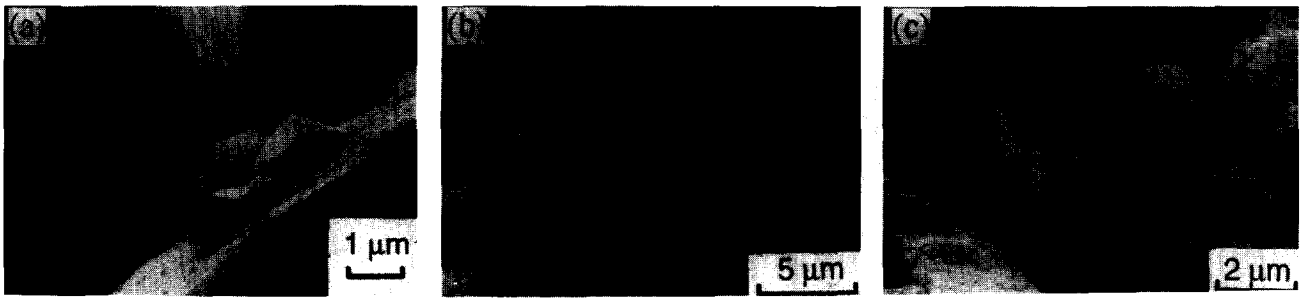

Fig. 4. SEM study of the $4BS_B$ sample after soaking at room temperature: (a) SEM showing the p_1-type particles with a coherent interface between $4BS_B$ and p_1 $PbSO_4$; (b) surface needle covered by p_2-type particles, and (c) needle's cross section showing the p_2-type layer thickness.

3.1.1. *Soaking of pure 4BS phases*

At room temperature, soaking of the $4BS_B$ sample clearly reveals two growth mechanisms leading to two kinds of $PbSO_4$ particles.

The first type of particles (called p_1) appear at the beginning of the reaction as polyhedral particles whose average size reaches 2 µm at the end of reaction. SEM (Fig. 4(a)) indicates that the nucleation of these crystals takes place at the surface of the needles, with a coherent interface between the two phases (4BS and $PbSO_4$). The presence of these particles results from a dissolution/recrystallization process. The smallest particles, in the form of broken needles, easily dissolve in the sulfuric acid solution whereas polyhedral new crystals grow by feeding from the solution at the surface defects of the biggest needles.

The second type of particles (called p_2) are produced by the slow transformation of the $4BS_B$ needles: at the beginning of the reaction, the surface of the needles appears as granular but after a long soaking time, a multitude of small $PbSO_4$ particles appears (Fig. 4(b)). Observations of their cross section (Fig. 4(c)) show that the needle sulfation proceeds from the surface towards their centre, in agreement with the Lam results [8]. By this second sulfation process, a layer of small agglomerated $PbSO_4$ nodules whose size does not exceed 0.2 µm is obtained, but the overall shape of the starting needles is retained.

For the $4BS_C$ sample, the same soaking mechanisms are observed with two populations of $PbSO_4$ crystals (Fig. 5). However, the p_1-type crystals (2 µm) resulting from the dissolution/recrystallization process are much more numerous than for the $4BS_B$ sample. This fact is probably due to the larger number of defects in the form of carbonate impurities located at the needle surface when they are produced by curing; indeed these conditions favour the growth of carbonated phases at the needle surface if the CO_2 level is not controlled during curing.

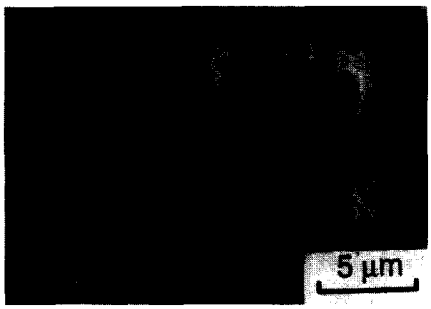

Fig. 5. SEM study of the $4BS_C$ sample after soaking at room temperature showing the p_1- and p_2-type of PbSO4 particles.

The soaking experiments performed at 55 °C confirm the existence of the two types of sulfation mechanism, independently of the nature of the 4BS precursor. Increasing the temperature only results in an enhancement of the reaction rate but does not modify the upper limit of the size achieved for each kind of $PbSO_4$ crystals (0.2 and 2 µm). The $4BS_B$ needles are fully transformed in the two $PbSO_4$ populations after 24 h of soaking at 55 °C (Fig. 6(a)) while several days are needed at room temperature. In the case of the $4BS_C$ sample, the complete transformation of the needles cannot be achieved (Fig. 6(b)) because the maximum thickness of the $PbSO_4$ layer (1.5 µm) is much smaller than the cross section of the $4BS_C$ needles (10 µm). These results are consistent with those of Lam et al. [10] who noticed that the $PbSO_4$ layer levels off to a value near 2 µm. However, the layer thickness depends on the temperature and the duration of

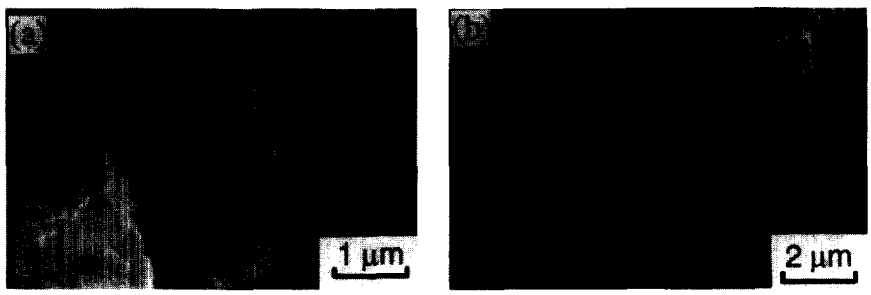

Fig. 6. Soaking of the $4BS_B$ and $4BS_C$ at 55 °C: (a) a complete transformation of $4BS_B$ smples is observed after 24 h, and (b) for the $4BS_C$ sample, the maximum thickness of the $PbSO_4$ layer is 1.5 µm.

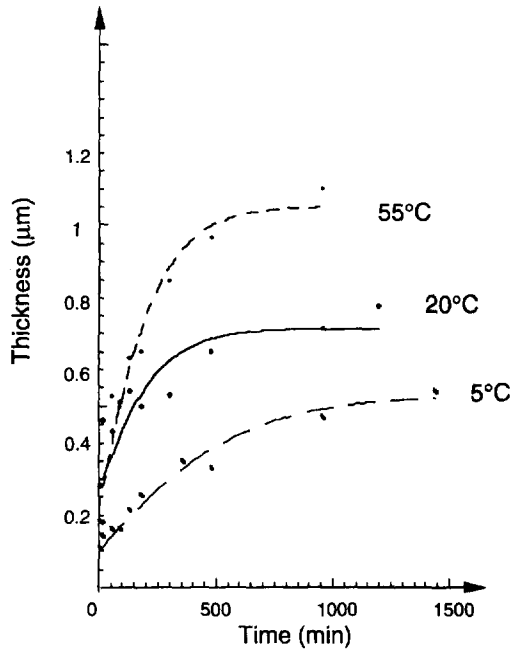

	Value (5°C)	Value (20°C)	Value (55°C)
a1	-62.130	-7.7836	-3.9437
a2	0.53427	0.81386	1.0957
a3	-3056.5	-770.27	-378.82
a4	606.49	284.62	229.67
Chisq	0.00214	0.01033	0.00615

Fig. 7. Soaking of the $4BS_B$ sample. Thickness of the p_2-type of the $PbSO_4$ layer vs. time at 5, 20 and 55 °C, see text.

soaking. Fig. 7 shows the thickness versus time curves at 5, 20 and 55 °C. Fitting of these curves indicates that the $PbSO_4$ growth seems to be controlled by the following law

$$y=(a_1-a_2)/\{1+\exp[(t-a_3)/a_4]\}+a_2 \quad (1)$$

where y is the thickness and a_1, a_2, a_3 and a_4 are constant values, and t is the soaking time.

3.1.2. *Formation of 4BS pure phases*

This part only deals with the formation results of the 4BS phase prepared by Biagetti's method ($4BS_B$). Indeed, the behaviour of the $4BS_C$ sample prepared by curing of 3BS is quite similar to that of the 4BS phase involved in the industrial plates for which detailed results are given in Section 2.

Fig. 8 shows the variations of the 4BS, $PbSO_4$, and PbO_2 molar ratios versus the charge time for various experimental conditions: formation with a very short soaking time (less than 1 min) at 20 and 55 °C (Fig. 8(a) and (b)) and formation at 20 °C after soaking during 6 h (Fig. 8(c)). These curves reveal two main stages for the oxidation kinetics. During a first stage, the oxidation reaction is very slow and the PbO_2 amount remains very low, while 4BS transforms into $PbSO_4$ so that the $PbSO_4$ molar ratio increases. After this period, the oxidation kinetics strongly increase as shown by the slope change of the PbO_2 curve. This behaviour can be explained as follows:

(i) As the oxidation starts near the current collector and progresses towards the electrolyte interface (see SEM study) the oxidation reaction first requires the diffusion of the sulfuric acid through the very compact pellet of active material. Moreover, the oxidation of the pellet takes place only after the oxidation of the sulfated lead foil used as current collector is complete. Thus, both acid diffusion and collector oxidation predominate over the active material oxidation during the first period resulting in a delay of the charge reaction. Comparison of Fig. 8(a) and (b) shows that the delay is shorter at 55 than at 25 °C, as expected.

(i) Finally, these curves strongly suggest that $PbSO_4$ is an intermediate to the oxidation reaction as previously mentioned by Lam et al. Indeed, without a prior soaking period (Fig. 8(a) and (b)), the amount of $PbSO_4$ remains relatively high throughout formation suggesting that two reactions occur simultaneously

$$4BS \rightarrow PbSO_4 \quad (2)$$

$$PbSO_4 \rightarrow PbO_2 \quad (3)$$

With a prior soaking period of 6 h (Fig. 8(c)), reaction (2) is nearly complete before starting the charge so that reaction (3) strongly predominates during formation. Consequently, $PbSO_4$ disappears and the amount of PbO_2 is increasing.

The SEM study gives further information on the role of the intermediate $PbSO_4$ phase during formation.

At the beginning of the second period (150% of charge) at 25 °C, the needles near the collector that have been partly converted into the p_2-type of $PbSO_4$ crystals are already oxidized, while the biggest polyhedral $PbSO_4$ particles (p_1) remain unaffected (Fig. 9(a)). Near the electrolyte interface, PbO_2 is not detected and the needles are found to be sulfated (Fig. 9b) into p_2-type of $PbSO_4$ crystals. At the final stage of formation (400% of charge), all the 4BS needles show at their surface a thin fibrous microporous layer of PbO_2 crystals with large fissures crossing through this layer (Fig. 10(a)). These cracks permit acid diffusion inside the needles, thereby leading to oxidation of the needle centre into PbO_2, with a morphology different from the crust (Fig. 10(b)). At 55 °C, the same process is involved but the resulting interconnected small PbO_2 crystals are thicker thereby giving a more rigid skeleton without fissures (Fig. 11(a) and (b)).

A last point worth mentioning is that the p_1-type of $PbSO_4$ particles are found to be oxidized only at the final stage of formation. Such behaviour can be ascribed to the large particle size of these crystals (1–2 µm against 0.2 µm for p_2) that makes oxidation difficult.

It can be concluded that the PbO_2 crystal growth mainly takes place on the p_2-type of the interconnected $PbSO_4$ particles at the needle surface through a metasomatic process following the metasomatic $4BS \rightarrow p_2\text{-}PbSO_4$ transformation as evidenced in the first part. This double metasomatic process leads both at 20 and 55 °C to a very suitable macroskeleton because of its high porosity and surface area. However, the thickness of the individual PbO_2 grains depends on the formation temperature. For the very thin intercon-

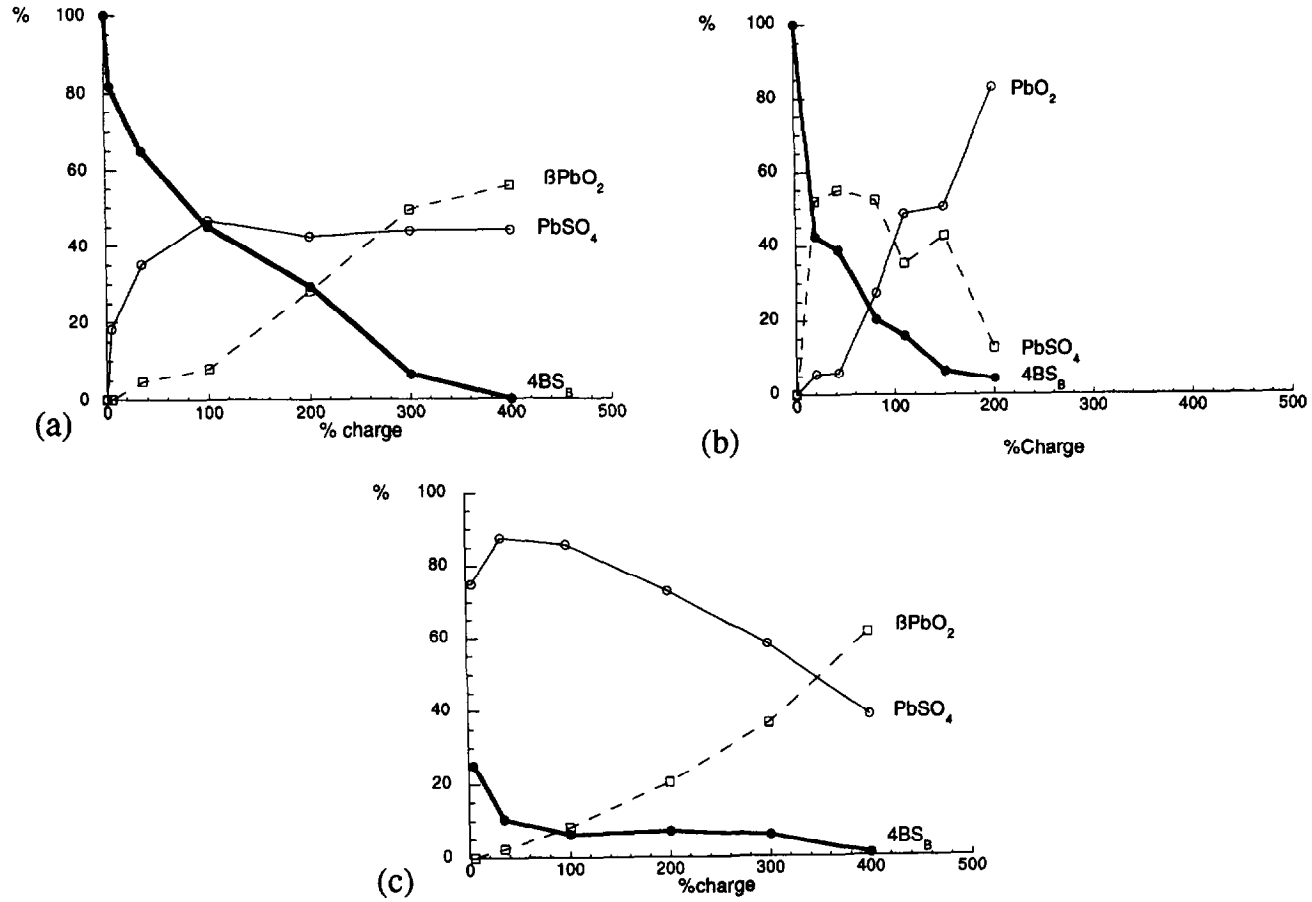

Fig. 8. Variation of the 4BS, $PbSO_4$ and PbO_2 molar ratios vs. charge time: (a) very short soaking time (<1 min) at -20 °C; (b) very short soaking time (1 min) at -55 °C, and (c) pre-soaking time of 6 h at -20 °C.

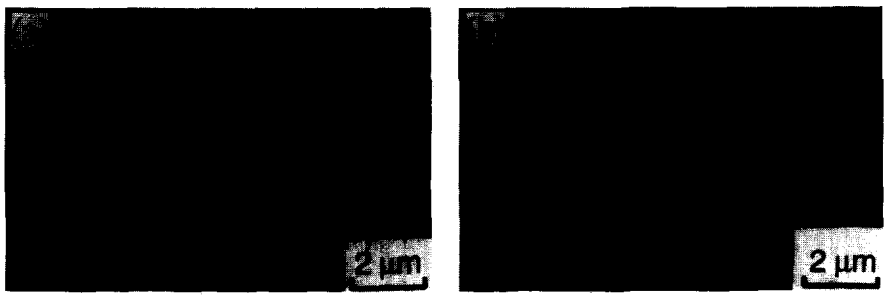

Fig. 9. Formation of the $4BS_B$ sample at 150% of charge: (a) needles oxidized to PbO_2 near the current collector, and (b) sulfated needles at the electrolyte interface.

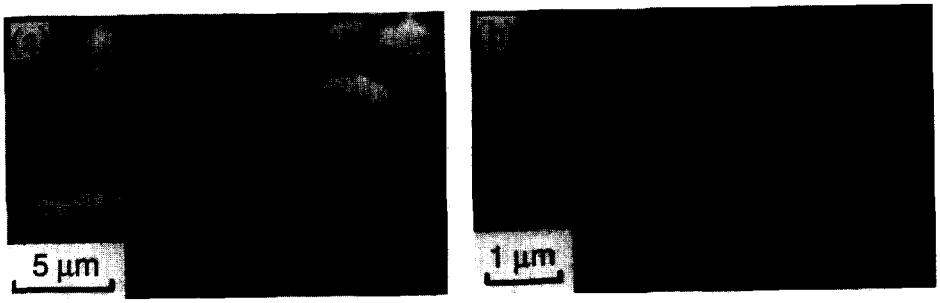

Fig. 10. Formation of the $4BS_B$ sample at 20 °C. SEM graphs of the active material at 400% of charge: (a) fully transformed needles showing large fissures in the PbO_2 crust, and (b) cross section of a fissured needle showing the needle centre transformation into active mass with different textural features from the crust.

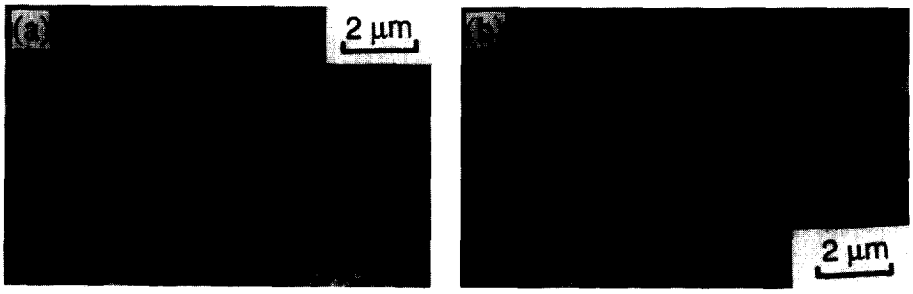

Fig. 11. Formation of the $4BS_B$ sample at 55 °C: (a) needle surfaces covered by interconnected PbO_2 crystals thicker than those obtained at 20 °C, and (b) cross section of the needles.

nected PbO_2 crystals obtained at 20 °C, the relaxation of the strains induced by the p_2-$PbSO_4 \rightarrow PbO_2$ needle transformation is associated with the formation of fissures in the PbO_2 crust. In contrast, the thicker skeleton characterizing the 55 °C active material makes the strain relaxation easier, i.e. without fragmentation.

3.2. Soaking and formation of 4BS plates

3.2.1. Soaking

As for the investigation on the pure 4BS phases, the soaking of 4BS plates from industrial manufacturing was performed at room temperature and at 55 °C prior to the investigation of the formation step. In some cases, we made the comparison with the 3BS positive material treated in a similar manner.

The chemical compositions of 4BS plates before formation in relation to the soaking time are given in Fig. 12.

On this graph it is observed that the sulfation is not completed even after a long soaking time. As expected, the total sulfation is difficult to achieve because of the large dimensions of the 4BS crystals. SEM of the 4BS industrial soaked plates confirm the results of Section 3.1.1. After 0.5, 2 and 5 h of soaking at 55 °C (Fig. 13(a)), the crystal 4BS surface appears to be entirely covered with 1–2 µm polyhedral particles (p_1-$PbSO_4$) so that p_2 crystals are not observed, except for cross-section images (Fig. 13(b)). If we compare these SEM graphs with those of Figs. 4 and 5, it appears that the p_1-type crystals are more numerous for industrial plates than for the pure phases. We assume that much more residual PbO, defects and/or carbonated species are present in the industrial plates thereby promoting the p_1-type particle growth. After 5

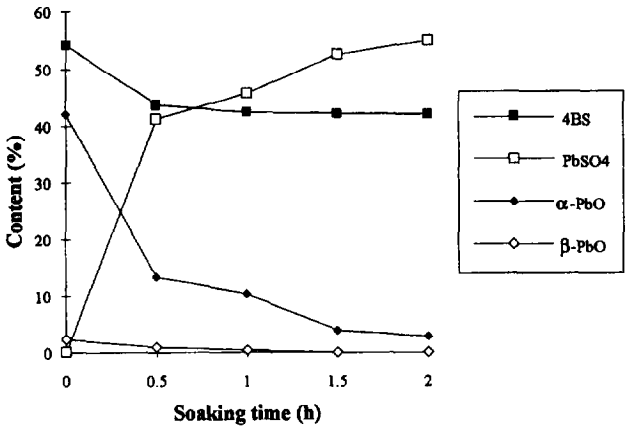

Fig. 12. Phase composition of 4BS plates vs. soaking time.

h of soaking, the 4BS large crystals remain mainly unconverted even at 55 °C (Fig. 13(b)). This is due to the hindrance of transport through the p_2 dense layer which reaches a limited thickness of ≈ 0.7 and ≈ 1.25 µm for $T = 25$ and 55 °C, respectively.

The sulfated active mass evolution during soaking (Fig. 14) is also in good agreement with a sulfation mechanism in two stages: the first stage is fast and corresponds to the 4BS crystal surface sulfation (appearance of p_1-$PbSO_4$). The second stage, occurring after 30 min, is slow because of the metasomatic process leading to 0.2 µm interconnected $PbSO_4$ nodular grains p_2.

In order to correlate these results to the active material surface modifications, porosity measurements have been made. It is shown in Table 1 and Fig. 15 that the total porosity is not much modified by the soaking time. This behaviour can be related to the unchanged needle shape during soaking

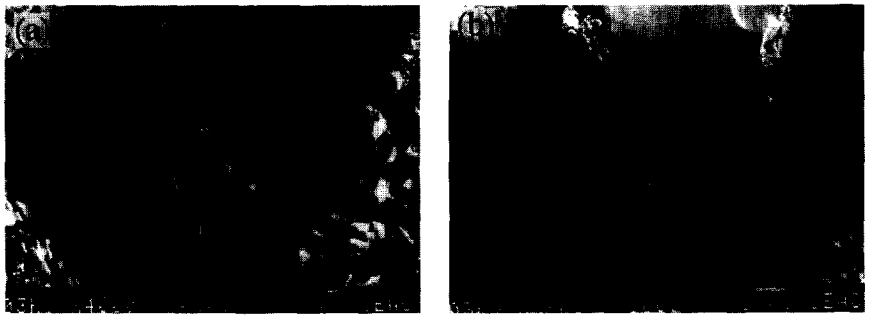

Fig. 13. SEM of the soaked needle of 4BS at 55 °C after 5 h of soaking: (a) needle covered by numerous p_1-type of $PbSO_4$ crystals, and (b) cross section of a needle showing the unconverted inner 4BS phase together with the p_1- and p_2-type of the $PbSO_4$ crystals on the crust.

Table 1
Porosity measurements for 4BS active material after various soaking times

Soaking time (h)	Total porosity ($cm^3 g^{-1}$)	Mean pore radicals (μm)	Pore surface ($m^2 g^{-1}$)	Absorbed SO_4 (g per 10 g positive active mass)
0	0.117	1.5	0.3	0
0.5	0.098	0.15	2.31	0.55
2	0.084	0.33	1.42	0.62
5	0.086	0.91	0.72	0.8

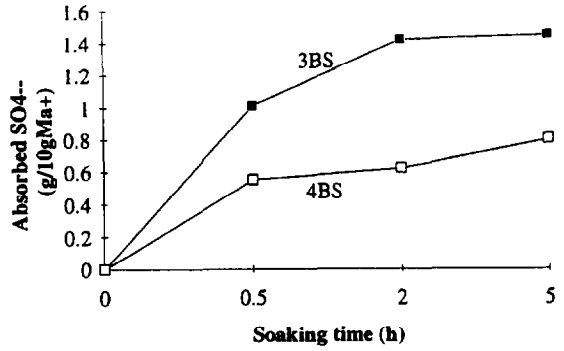

Fig. 14. Absorbed sulfate (g per 10 g PAM) evolution of 4BS and 3BS plates vs. soaking time.

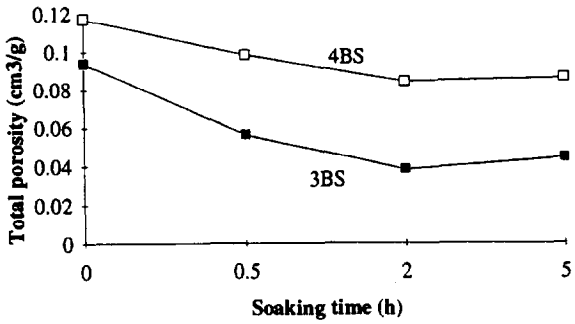

Fig. 15. Total porosity evolution for 4BS and 3BS plates vs. soaking time.

which defines a stable macroporous structure. Nevertheless, the mean pore radius decreases during the first hour, and then increases with the soaking time. The pore surface evolution is the opposite. After a long soaking time, these two parameters seem to return to their initial values (to those before sulfation). This behaviour is rather complicated to explain, as a complex sulfation mechanism is involved. We assume that the plate structure is strongly modified at the beginning of soaking due to the p_1-$PbSO_4$ particles precipitation at the 4BS needle surface. This would explain the mean pore radius decrease. However, the subsequent growth of the p_1 particles which rapidly reach 2 μm in diameter again favours the mercury penetration leading to an increase in the mean pore diameter in a second stage.

Finally, it is interesting to compare the 4BS and 3BS behaviour during soaking while using similar experimental conditions. On Figs. 14 and 15, it is well shown that the total porosity and the sulfation rates are rather different for both salts. We conclude that the industrial process approach for soaking of small 3BS and large 4BS must not be performed in the same way. The 4BS soaking time and corresponding temperature should be sufficiently high to have a suitable growth of p_2-$PbSO_4$. In contrast, the 3BS soaking time and temperature should be low. Indeed, as will be reported in a following paper, the 3BS soaking has been proved to produce, at a high rate, $PbSO_4$ grains similar to p_1, for which oxidation is difficult. Consequently, the shorter is the soaking time, the easier is the 3BS plate oxidation.

3.2.2. *Formation of 4BS plates*

The chemical compositions of 4BS plates after 140% formation in relation with the soaking time are given in Table 2. It is evident that there is an increase of the final PbO_2 content with soaking times larger than 30 min. This increase can be evaluated by X-rays between 15 and 20% for 2 h of soaking. The wet chemical analysis confirms this evolution but the PbO_2 contents are found to be systematically higher (5–10%). The formed material likely presents a high content of poorly crystallized PbO_2 as explained by Pavlov [11] due to the presence of amorphous PbO_2 in hydrated regions.

Fig. 16 allows for the comparison of the 4BS crystal cross sections after formation until 143%, for short and long soaking times. At long soaking time, the external layer consists of PbO_2 with a very fine texture resulting from p_2 oxidation; the second layer is probably p_2-$PbSO_4$ and the interior layer is the unconverted 4BS. Voids are observed at the PbO_2/$PbSO_4$ interface as a result of the large difference in density between these two phases. The same layers are observed with short soaking duration but the PbO_2 thickness is smaller and a remaining amount of p_1 unformed crystals appears as an fourth external layer. Large fissures crossing through the PbO_2 layer are not observed, as in the case of the pure 4BS

Table 2
Phase composition of the formed 4BS plates (250% of charge at $C/20$ rate) after different soaking times

Conditions	Chemical composition (peaks %)		
	β-PbO_2	$PbSO_4$	4BS
Without soaking	51.3	43.3	5.4
Soaking time, 0.5 h	52.1	27.7	20.1
	52.3	34.5	13.2
Soaking time, 2 h	63	27.7	8.1
	68.8	13.8	16.9
Soaking time, 4 h	64	8.8	27.1
	68.9	21.3	9.9

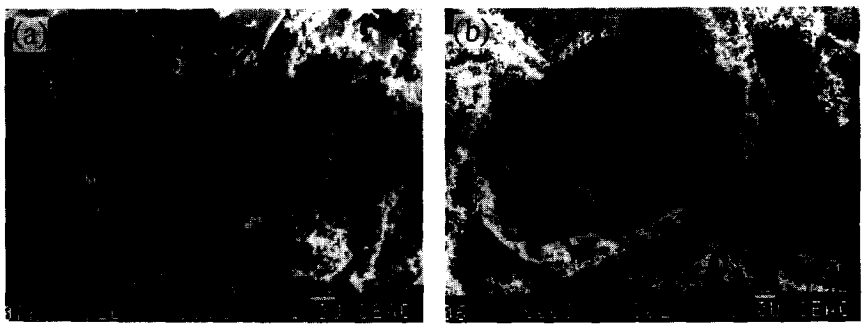

Fig. 16. SEM of formed needle cross sections of 4BS: (a) 0.5 h soaking, and (b) 2 h soaking.

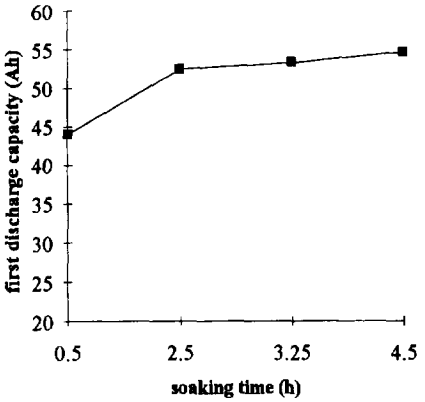

Fig. 17. Evolution of the first discharge capacity of a complete battery in relation to the soaking time before the formation.

phase formation at 55 °C probably due to the lower charge (143% instead of 400%).

In order to evaluate the battery performance as a function of the soaking duration, capacities were evaluated on batteries for which 4BS positive plates have been formed after different soaking times, using a complete formation at 550 Ah kg^{-1} (250% of the theoretical capacity) during 48 h ($R=0.24$ Ah^{-1} kg^{-1}). Results of first discharge $C/20$ capacities (based on 120 Ah kg^{-1} nominal capacity) are reported in Fig. 17. This figure clearly indicates that the first discharge capacity increases with soaking time as expected from the increasing PbO_2 content.

These observations are in good agreement with the requirement of having p_2 species for oxidation into PbO_2 as shown in Section 3.1.1. During formation, four reactions compete: (i) $4BS \rightarrow p_1$; (ii) $4BS \rightarrow p_2$; (iii) $p_2 \rightarrow PbO_2$, and (iv) $p_1 \rightarrow PbO_2$. From the results of Section 3.1.1 it has been shown that the sequence in which these reactions proceed is as follows: (iv) occurs when (iii) is fairly completed. Moreover, (iii) takes place only if transformation (ii) has been partly observed. It is therefore not surprising that the highest levels of PbO_2 are obtained with long soaking times for which transformation (iii) is possible from the beginning of formation. However, these conclusions should be used with care since in real industrial conditions the acid/material ratio may be different and the p_2 species could not reach high levels for low acid/material ratios. This is often the case in valve-regulated lead/acid batteries.

4. Conclusions

We clearly pointed out that the oxidation of lead tetrabasic mass to PbO_2 proceeds through the growth of $PbSO_4$ crystals of different morphology (large polyhedral particles (p_1 = 2 μm) and small interconnected particles ($p_2 = 0.2$ μm).

The first p_1-type crystals recrystallize by liquid processes from small 4BS or residual PbO which are very rapidly sulfated at the beginning of the soaking. The second p_2-type species result from the slow transformation of the 4BS needle into $PbSO_4$ via a metasomatic process owing to the slow diffusion of sulfate ions and water through the growing $PbSO_4$ layer.

Thus, the formation step that strictly concerns the oxidation of $PbSO_4$ to PbO_2 was also found to proceed in two different ways, depending on the $PbSO_4$ morphology.

The oxidation of p_2 at the 4BS needle surface starts first and provides β-PbO_2 with a very fine microporous structure. The reaction mechanism is again metasomatic, then the microporosity and the crystal interconnection are maintained through the mass leading to a good utilization of the positive active material and capacity loss should be delayed.

The double metasomatic process $4BS \rightarrow PbSO_4 \rightarrow PbO_2$ has been observed at 25 and 55 °C, so that the same active material macrotexture is involved for both temperatures (interconnected thin $PbSO_4$ crystals showing needle-shape aggregation). Temperature was only found to affect the microtexture of PbO_2 interconnected crystals: the individual PbO_2 grain appears thicker at 55 °C, so that a more rigid skeleton is obtained, limiting the crack formation through the PbO_2 needle crust.

When p_2 species oxidation slows down due to the limitation of exchanges through the $PbSO_4$ layer, the oxidation of p_1 starts. From this fact, the 4BS crystals' cores and large polyhedral $PbSO_4$ particles are much difficult to convert into PbO_2.

The same conclusions can be drawn from observations obtained with plates from standard manufacturing. Long soaking times combined with relatively high temperature (55 °C) are necessary for 4BS conversion to p_2 and, therefore, to obtain a good plate formation. $C/20$ discharges measured on full batteries confirm this observation.

Acknowledgements

The authors thank the 'Agence de l'Environnement et de la Maîtrise et de l'Energie' (ADEME) for its financial support.

References

[1] J. Burbank, *J. Electrochem. Soc.*, *113* (1966) 10.
[2] R.V. Biagetti, *Bell Syst. Tech. J.*, *49* (1970) 1305.
[3] K.R. Bullock, B.K. Mahato and W.J. Wruck, *J. Electrochem. Soc.*, *138* (1991) 3545.
[4] D. Pavlov and N. Kapkov, *J. Electrochem. Soc.*, *137* (1990) 16.
[5] D. Pavlov, G. Papazov and V. Iliev, *J. Electrochem.*, *119* (1972) 8.
[6] D. Pavlov and E. Bashtavelova, *J. Power Sources*, *31* (1990) 243.
[7] B. Culpin, *J. Power Sources*, *25* (1989) 309.
[8] L.T. Lam, H. Hozgun, L.M.D. Cranswick and D.A.J. Rand, *J. Power Sources*, *42* (1993) 55.
[9] F. Vallat-Joliveau, A. Delahaye-Vidal, M. Figlarz and A. de Guibert, *J. Power Sources*, *55* (1995) 97.
[10] R.J. Hill, A.M. Foxworthy and R.J. White, *J. Power Sources*, *32* (1990) 315.
[11] D. Pavlov, *J. Power Sources*, *46* (1993) 171.